Saudi Journal of Biological Sciences 28 (2021) 840–846

Contents lists available at ScienceDirect

Saudi Journal of Biological Sciences

journal homepage: www.sciencedirect.com

Original article

Spectral characterization of hydroxyapatite extracted from Black Sumatra and Fighting cock bone samples: A comparative analysis

K.C. Vinoth Kumar [a,*], T. Jani Subha [b], K.G. Ahila [c], B. Ravindran [d], S.W. Chang [d], Ahmed Hossam Mahmoud [e], Osama B. Mohammed [e], M.A. Rathi [f]

[a] Department of Physics, Udaya College of Arts and Science, Udaya Nagar, Ammandivilai, Kanyakumari, Tamil Nadu, India
[b] Department of Chemistry, Rohini College of Engineering & Technology, Anjugramam, Kanyakumari, Tamil Nadu, India
[c] Department of Biotechnology, Udaya College of Arts and Science, Udaya Nagar, Ammandivilai, Kanyakumari, Tamil Nadu,India
[d] Department of Environmental Energy and Engineering, Kyonggi University Youngtong-Gu, Suwon, Gyeonggi-Do 16227, South Korea
[e] Department Zoology, College of Science, King Saud University, P.O Box 2455, Riyadh 11451, Saudi Arabia
[f] Department of Biochemistry, Sree Narayana Guru College, Coimbatore 641 105, Tamil Nadu, India

ARTICLE INFO

Article history:
Received 5 September 2020
Revised 25 October 2020
Accepted 1 November 2020
Available online 11 November 2020

Keywords:
Black Sumatra
Fighting cock
Hydroxyapatite
FTIR
XRD
SEM

ABSTRACT

At present, chicken business is occupying a major portion in the market and huge amount of bone wastes are dumped into the open places lead in environmental pollution. In this analysis, natural hydroxyapatite was extracted by thermal calcination process at different temperature ranges from 700 °C, 900 °C and 1100 °C and compared its spectral characteristics. The crystalline nature, functional groups and morphological characteristics of hydroxyapatite obtained from both bone samples were studied using XRD, FTIR and SEM analysis. The crystallite size, lattice parameters, specific surface area, volume and degree of crystallinity were measured using XRD data. The mean grain size of Black Sumatra and Fighting Cock bone hydroxyapatite was 62.67 nm and 31.34 nm respectively. The FTIR spectrum showed major peaks at 634.58 cm^{-1} and 470.63 cm^{-1}, 1413.82 cm^{-1} and 1460 cm^{-1} indicates the presence of carbonate group and phosphate groups in both samples. The SEM micrograph confirmed the existence of maximum pores in matrix of fighting cock bone than Black Sumatra bone sample. Thus, the comparative analysis concluded that nano-sized hydroxyapetite obtained from bone wastes of fighting cock can be utilized as a low-cost biomaterial for the production of various implant coating materials and substitute for ceramics in bones and dentistry applications.

1. Introduction

Recently, the utilization of waste obtained from natural resources is playing a crucial role in the production of value-added products and bio-based implant materials for medical applications (Mohd Puad et al., 2019). On the other hand, the pollution caused by bio-wastes is drastically mounting due to open disposal in the environment. The reuse of biowastes for preparing valuable biomaterials is an efficient route to reduce pollution and show an efficient way for a solid waste management system as well as sustainable growth of economy (Ronan and Kannan, 2017). Bones are naturally composed of organic material typically type I collagen (20%), inorganic materials consist of hydroxyapetite (70%) and 10% have been occupied by water content (White and Best, 2007). The hydroxyapatite (Ca_{10} $(PO_4)_6$ $(OH)_2$), abbreviated as HAp belongs to apatite family. It is a type of biologically active calcium phosphate based bioceramic, non-toxic, non-mutagenic, non-allergic, immunologically inactive biomaterial of bones. It can be used as an efficient implant material and bone substitute because of its biocompatibility and excellent osteoconductivity nature (Komlevet al., 2001; Rezakhani and Motlagh, 2012). In addition to this, HAp materials are thermodynamically stable at physiological condition and it strongly engaged in bone bonding and facilitates bone repair mechanism (Mondal et al., 2012).

Natural HAp can be exists in two forms such as A-type and B-type. A-type carbonated HAp materials substituted with a hydroxyl group (OH^-) and B-type carbonate HAp substituted by a phosphate

* Corresponding author.
E-mail address: kcvinodhkumar@gmail.com (K.C. Vinoth Kumar).
Peer review under responsibility of King Saud University.

Production and hosting by Elsevier

https://doi.org/10.1016/j.sjbs.2020.11.020
1319-562X/

group ($PO4^{3-}$), which resembles the biological apatite (Huang et al., 2010; Leventouri, 2006). The occurrence of ions highly influences the structural, optical and morphological properties of HAp materials (Londono-Restrepo et al., 2018). In human bones, hydroxyapatite materials are found as impure form due to the incorporation of other elements, which are involved in bone metabolism (Supova et al., 2011). It has been found to play a vital role in various fields including drug delivery (Barabas et al., 2019), orthopedics, dentistry, maxillofacial (Balamurugan et al., 2008) bone and tissue engineering (Senthilarasan et al., 2014). Researchers have been also reported the textile dye decolorizing efficiency of naturally derived hydroxyapatite (Hubaidillah et al., 2020; Adeogun et al., 2018; El Boujaady et al., 2016).

Biocompatible hydroxyapetite can be derived from several natural sources includes cow bones (Hubaidillah et al., 2020), pig, goat, chicken bones (Ramesh et al., 2018; Harahap et al., 2017; Supova et al., 2011), egg shell (Ronan and Kannan, 2017), aquatic sources such as fish bone, fish scales, coral (Mondal et al., 2012) also from plants and algae (Mohd Puad et al., 2019). Several physical and chemical methods are adopted for the preparation of synthetic and bio-based HAp and their properties and the ratio of chemical components are more similar to naturally available HAp and also excellent human adaptability and biocompatibility. Traditionally, HAp can be synthesized by microwave irradiation (Yang et al., 2002), thermal (Rajesh et al., 2012), Sol-gel method, precipitation (Harahap et al., 2017), hydrothermal techniques (Alif et al., 2018) etc. Black Sumatra chicken is a long-lived breed and originated from Java and Borneo. Fighting cocks is belongs to Aseel breed distributed around the world. These varieties are widely used for fighting purposes because of their pugnacity. The present research is aimed to compare the spectral characteristics of hydroxyapatite obtained from bone wastes of two chicken varieties such as Black Sumatra and Fighting cock by XRD, FTIR and SEM analysis. The spectral measurements facilitate to generate biocompatible, stable, low cost and efficient biomaterial from bio-wastes for medical applications.

2. Materials and methods

2.1. Preparation of bone samples

Raw bone samples of Black Sumatra and Fighting cock were collected from the local slaughter house and a poultry farm. The chicken bones were boiled with water for 1 h to remove fat (defatting) content and macroscopic adhering impurities. After this process, the bones were washed and cleaned thoroughly to remove all attached meat, bone marrows and soft tissues. Cleaned defatted bone samples were immersed in acetone for deproteination process for 2 h and washed with water. The deproteinized product was kept in the oven at 80 °C to evaporate the water content (Murugan et al., 2006). The dried chicken bones were crushed into small pieces using mortar and pestle and then milled into smaller particles by rotary mill.

2.2. Calcination of bones

In calcination process, accurately weighed 20 g of both bone particles were taken in two alumina crucibles and kept in a Muffle furnace for thermal process. This process was conducted at different temperature, such as 700 °C, 900 °C and 1100 °C for 3 h at heating rate 10 °C/min to eliminate organic constituents present in the bone and to recover hydroxyapatite (Barakat et al., 2009). The heated samples were cooled slowly to room temperature and stored for further analysis.

2.3. Spectral characterization of calcinated bones

The calcinated bone samples of Black Sumatra and Fighting cock were subjected to spectral characterization studies using instrumental techniques. The crystalline nature and lattice parameters were determined by XRD analysis (XRD-Bruker D8 advance). FTIR spectrum was recorded in the wavelength of infrared region ranges from 400 to 4000 cm^{-1} using Potassium bromide pellet method (Shimadzu- IR Tracer 100) and the morphological features were studied by Scanning electron microscope (Joel JSM 6390) operated at 20 kV with 400 Kx magnification.

3. Results and discussion

3.1. Extraction of hydroxyapatite

The deproteinized chicken bones samples were subjected thermal calcination process was to extract hydroxyapatite. Initially, the deproteinized bone powder was observed as pale yellow in colour. After the thermal treatment at varied temperature such as 700 °C, 900 °C and 1100 °C, colour variation was observed and the material become whitish colour due to the complete elimination organic components present in chicken bone powder. There was no visible colour change was observed after the temperature above 900 °C and 1100 °C. It might be due to the loss of organic content from the bone samples after 900 °C. Barua et al., (2019) also prepared pure phase of HAp particles from chicken bones wastes by thermal calcination process at 900 °C. Venkatesan and Kim (2010) reported the removal of organic compounds such as collagen and protein from fish bones during thermal calcination. Similarly, Ooi et al., (2007) also observed the loss of water and protein content from chicken bone powder after calcination process at varied temperature ranges from 30 °C to 500 °C.

3.2. XRD analysis of Black Sumatra and Fighting cock bone HAp

The XRD pattern of Black Sumatra bone sample is depicted in Fig. 1. The XRD spectrum showed intense diffraction peak at the 2θ angle regions with the intensity 26.2592°, 29.2448°, 32.2435°, 32.5316°, 33.2780°, 34.4827°, 40.1658°, 47.0536°, 48.3762°, 49.7381°, 50.9428°, 51.6892°, 52.4356°, 53.4831°, 56.1807°, 60.3519°, 62.0078°, 63.3566°, 64.4041°, 65.4517°, 72.0384°, 74.1335°, 77.5905°, 77.5905° and 78.6381° corresponding to the

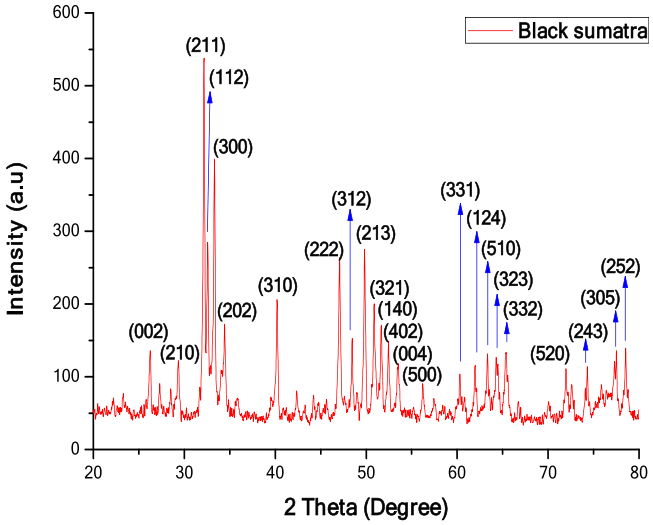

Fig. 1. XRD pattern of Black Sumatra bone HAp.

crystal planes denoted by Miller indices (002), (210), (211), (112), (300), (202), (310), (222), (312), (213), (321), (140), (402), (004), (500), (331), (124), (510), (323), (332), (520), (243), (305) and (252) respectively. The obtained intense peaks were matched with ICDD File.No.01-079-8093.

The crystallite structure of hydroxyapatite was hexagonal (Kumar et al., 2017) and the lattice constant parameters were calculated for (002) and (210) by the following formula (Equation (1)).

$$\frac{1}{d^2} = \frac{4}{3}\left[\frac{h^2 + k^2 + hk}{a^2}\right] + \frac{l^2}{c^2} \quad (1)$$

where 'd'is the Distance between adjacent planes; hkl refers to Miller indices planes.

The lattice constant values were found to be a = b = 9.2916 and c = 6.0. The average crystallite size of Black Sumatra chicken bone hydroxyapatite was calculated by Debye-Scherrer's equation and the average grain size was 62.67 nm.

$$D_n = \frac{0.9\lambda}{\beta \cos\theta} \quad (2)$$

The volume of hexagonal unit cell in hydroxyapatite was determined by the formula (Eq. (3)) (Webster et al., 2002). The volume of Black Sumatra chicken bone hydroxyapatite was 1019.63. This result was agreed with the reports of Rezakhani and Motlagh (2012).

$$V = 2.589 a^2 c \quad (3)$$

The specific surface area of chicken bone hydroxyapatite was calculated by the equation (4), (Palanivel and Rubankumar, 2013).

$$S = \frac{6 \times 10^3}{d \times \rho} \quad (4)$$

where crystallite size is denoted as 'ρ' and theoretical density of HAp is mentioned as'd' (d = 3.16 g/cm^3). The specific surface area was found to be S = 30.29.

The degree of crystallinity of the sample was calculated as X_c = 2.348544 by the equation (5).

$$X_c = (K/\beta)^3 \quad (5)$$

where K = 0.24 for HCP and β is FWHM values.

The XRD pattern (Fig. 2) of hydroxyapatite obtained from fighting cock bone powder showed the presence of intense peaks at the regions of 2θ angle at 26.2592°, 29.2448°, 32.2435°, 33.2780°, 34.4827°, 40.1920°, 47.0670°, 48.0670°, 49.8165°, 50.8577°, 51.6420°, 52.4715°, 53.5111°, 56.2426°, 60.2268°, 61.8638°, 63.3139°, 64.3774°, 65.4517°, 72.0384°, 74.2776°, 77.4203° and 78.4679° which corresponds to Miller indices crystal planes (002), (210), (211), (300), (202), (310), (222), (312), (213), (321), (140), (402), (004), (500), (331), (124), (510), (523), (332), (520), (243), (305) and (252) respectively. The obtained data was matched with ICDD File.No.01-079-8093. The characteristic peak, low crystalline quality has been reported for fight cock and the calculation of crystallinity percentage was carried out using the complete XRD pattern. The fighting cock bone hydroxyapatite also exhibit hexagonal structure. The lattice constant parameter a = 9.263 and c = 6 for (210) was calculated as per the Eq. (1). The mean grain size was determined as D_n = 31.34 nm by Debye-Scherrer's equation (2). The volume of the hexagonal unit cell of hydroxyapatite and specific surface area of fighting cock bone hydroxyapatite was found to V = 1490.10 and S = 60.585 respectively. The degree of crystallinity of the sample was calculated as respectively X_c = 0.762829 by the equation (5).

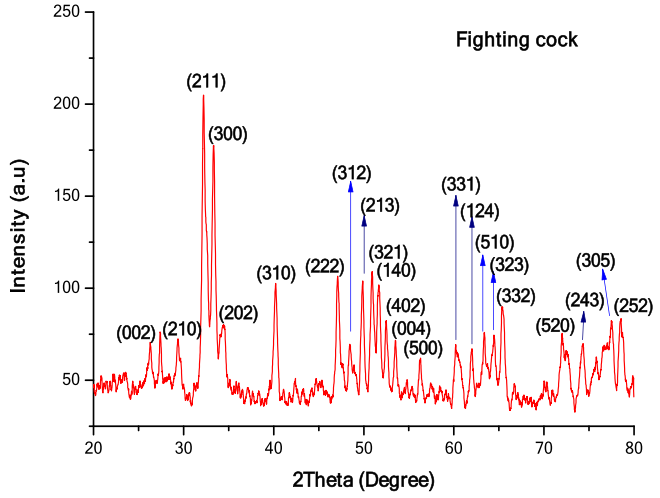

Fig. 2. XRD pattern of Fighting cock bone HAp.

The lattice constant parameters (a and c), the average grain size, volume of hexagonal unit, specific surface area and crystallinity values of both Black Sumatra and Fighting cock bone hydroxyapatite were determined using XRD patterns are summarized in Table 1.

The XRD patterns of both samples were compared and the findings clearly showed that the atoms are concentrated in Black Sumatra bone HAp than Fighting cock bone HAp. The peak intensity of same sample varied due to Miller indices (h k l) values. Basically, materials with higher Miller indices values take more time for the diffraction of X-ray beam. In both XRD patterns, the intensity of peaks at 2θ angle (32.2435° and 33.2780°) was higher for Miller indices planes (211) and (300). Furthermore, peaks of Fighting cock HAp were less sharp and broader which attributed to the reduction of crystalline size. However, XRD peaks of Black Sumatra HAp showed a substantial increase in height and width of peaks associated to the increment of crystallite size and crystallinity. Similar reports were reported by Ramesh et al., (2013) and Niakan et al., (2015). Fighting cock HAp showed the higher FWHM value than Black Sumatra HAp which indicates the poor crystallinity. The FWHM values also depend on the degree of crystallinity and size of the crystals were related with the purity of sample materials. The cyrstallinity and crystallite size of Fighting cock bone HAp was smaller when compared with Black Sumatra bone HAp. The resorption of hydroxyapatite in the bone, mainly depends on its crystalline size. Also, the amorphous phase of HAp materials can be easily absorbed by body fluids when it introduced into the body through HAp coated implants (Supova et al., 2011). The crystallite size of the HAp materials also imparts in the enhancement of hardness and mechanical strength and provides stability between the artificial or natural bone interfaces (Villacampa and Garcia-Ruiz, 2000). Furthermore, heating temperature applied during calcination treatment might be also significantly affects the crystallinity of HAp particles. Sun et al., (2013) reported the size of chemically synthesized HAp particles becomes stable after 600 °C.

Table 1
Parameters determined by XRD pattern.

Parameters	Black Sumatra	Fighting cock
Lattice constant parameters (**a** and **c**)	a = 9.2916; c = 6.0	a = 9.263 ;c = 6.8
Average grain size (D_n)	62.67 nm	31.34 nm
Volume of hexagonal unit (***V***)	1019.63	1490.10
Specific surface area (***S***)	30.29	60.585
Crystallinity (X_c)	2.348544	0.762829

3.3. FTIR spectral analysis

The FTIR spectrum of hydroxyapatite extracted from Black Sumatra bone and Fighting cock bone samples by thermal process is shown in Figs. 3 and 4. The identified functional groups are given in Table 2 and 3. The appearance of peaks 634.58 cm^{-1}, 601.79 cm^{-1}, 570.93 cm^{-1} were due to the symmetrical stretching of a phosphate group ($PO4^{3-}$) indicates the presence of hydroxyapatite free of organic matter. The absence of organic content of bone was due to the calcinations process at higher temperature (above 700 °C). The characteristic bands at 3641.60 cm^{-1} and 3570.24 cm^{-1}, were assigned to stretching vibration of a hydroxyl group (OH^-). The resorption process and dissolution of bone have been assisted by a modest part of the hydroxyl groups (Pasteris et al., 2004). The intensity of OH— band was found to be decreased in both samples after thermal clacination treatment attributed to dehydroxylation process in extracted HAp materials (Ooi et al., 2007; Ye et al., 2009). The peaks observed in the regions at 2883.58 cm^{-1}, 2827.64 cm^{-1}, 2827.64 cm^{-1}, 2142.91 cm^{-1} and 1990.54 cm^{-1} were assigned to CH stretching (Methyne), N—CH_3 (Methylamine), C═C Stretching (Alkynes) and overtone combination bands respectively. The bands at 1460.11 cm^{-1} and 1413.82 cm^{-1} were attributed to CO_3 Asymmetric stretching (carbonate group). The carbonate content in higher concentration helps in solubility and resorbability process occurs in bone (Wopenka and Pasteris, 2005). The characteristic absorption band found at 634.58 cm^{-1} corresponding to PO_4 bending (Phosphate group) and the presence of stretching vibrational phosphate groups were confirmed by the formation of the peaks at the regions 570.93 cm^{-1} and 470.63 cm^{-1} were observed in calcinated bone powders of Black Sumatra and fighting cock chickens.

The intensity of peaks for carbonate and phosphate group was found to be strong followed by hydroxyl group. The existence of well-defined peaks at 634.53 cm^{-1}, 470.63 cm^{-1} and 570–569 cm^{-1} authenticated the crystalline nature of HAp extracted from two varieties of chicken bones by thermal calcinations process (Venkatesan and Kim, 2010; Luna-Zaragoza et al., 2009). The phosphate ratio was lesser in Fighting when compared to Black Sumatra bone HAp. Moreover, the distinct peaks found around 470.63–634.53 cm^{-1}, observed in the FTIR spectrum of Black Sumatra HAp signifies the higher crystalline order than Fighting cock sample. The lesser crystallinity order of Fighting cock bone HAp purely correlated with crystallinity index determined from XRD analysis.

3.4. SEM analysis

The surface morphological investigation of Black Sumatra and Fighting cock bone HAp was carried out by SEM analysis and the micrographs of are depicted in Figs. 5 and 6.The obtained results revealed the existence of porous architecture throughout the matrix of calcinated HAp of both bone samples. The entire surface morphology showed that almost all pores were exhibited in nanoscale array. The appearance of the porous network in the matrix might be due to the elimination of organic constituents of bone during thermal process (Ramesh et al., 2018). The porous nature of extracted HAp enhances the progression of cell proliferation and differentiation for proper tissue functioning (Joschek et al., 2000; Murugan and Ramakrishna, 2005). This porous structure with nano sized pores could be considered as an advantageous property of HAp extracted from Black Sumatra and Fighting cock bones for bone tissue engineering, dentistry and orthopedic applications. The SEM micrograph of Fighting cock bone HAp confirmed its high order porosity than Black Sumatra bone HAp, so that can be more biocompatible in nature. The porous nature and osteoinductive properties of HAp enhances its mechanical strength and also osteointegrative feature facilitates in good interaction of HAp-coated implants with osteoblastic cellas and bone morphogenetic proteins (Xiao et al., 2016; LeGeros, 2002). Gautier et al., (2000) utilized antibacterial-loaded HAp material as coating agent in the surgical implant materials in order to prevent bacterial as well as inflammatory reaction. Guimond-Lischer et al. (2016) studied the antibacterial properties of HAp doped with Ag against *E. coli* and *S. aureus*. In another research, Rajesh et al., (2012) prepared composite bone scaffold using chicken bone based hydroxyapatite with alginate.

According to Rajkumar et al., (2017) muscular contraction is higher in Aseel birds than other birds. Thus, they are used for fight-

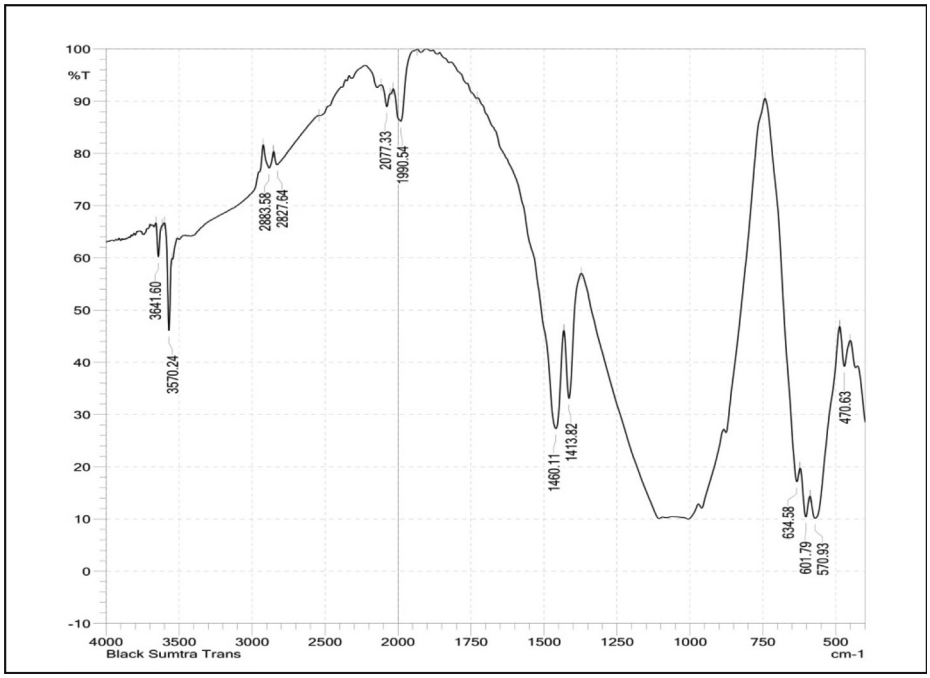

Fig. 3. FTIR spectrum of Black Sumatra bone HAp.

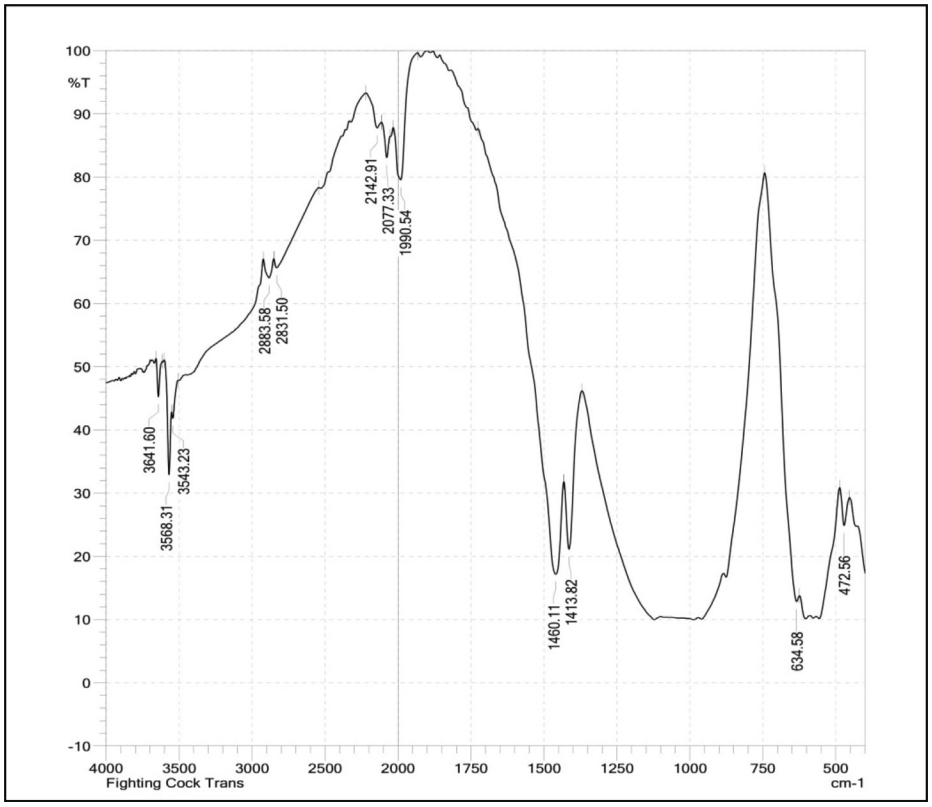

Fig. 4. FTIR spectrum ofFighting cock bone HAp.

Table 2
Characteristic bands of Black Sumatra bone HAP identified from FTIR spectrum.

Peaks (cm^{-1})	Stretching	Functional group
3641.60	OH vibration	Hydroxyl group
3568.31	OH Stretching	Hydroxyl group
3543.23	OH Stretching	Hydroxyl group
2883.58	CH Stretching	Methyne
2831.50	N—CH_3 CH stretching	Methylamine
2142.91	C═C stretching	Alkynes
2077.33	P—O bond	Phosphate group
1990.54	–	Overtone and combination band
1460.11	Asymmetric stretching	CO_3- groups
1413.82	CO_3	Carbonate group
634.58	PO_4 bending	Phosphate group
470.63	P-O stretching	Phosphate group

ing purposes. The mineral phase components such as Hydroxyapatite, dicalcium phosphate, calcium phosphate provide mechanical support to the bones and strengthening the muscular contraction (Rivera-Munoz, 2011). This might be the reason for the presence of more efficient HAp molecules in Fighting cock which enhances its bone strength than Black Sumatra. However, the mechanical integrity of processed material might be lost due to the removal of organic matters; thereby, this kind of HAp materials can be used for low-weight bearing bone grafting and coating on bio-implants.

Table 3
Characteristic bands of Fighting cock bone HAP identified from FTIR spectrum.

Peaks (cm^{-1})	Stretching	Functional group
3641.60	OH vibration	Hydroxyl group
3570.24	OH Stretching	Hydroxyl group
2883.58	CH Stretching	Methyne
2827.64	N—CH_3 CH stretching	Methylamine
2077.33	P—O bond	Phosphate group
1990.54	–	Overtone and combination band
1460.11	CO_3 Asymmetric stretching	Carbonate group
1413.82	CO_3	Carbonate group
634.58	PO_4 bending	Phosphate group
601.79	P═S Stretching	Phosphate group
570.93	P—O stretching	Phosphate group
470.63	P—O stretching	Phosphate group

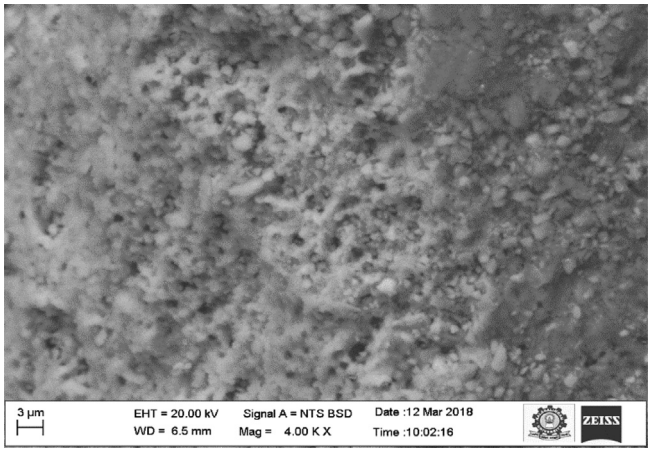

Fig. 5. SEM micrograph of Black Sumatra bone Hap.

4. Conclusion

In the present analysis, hydroxyapatite was extracted from the bones of two chicken varieties such as Black Sumatra and Fighting cock via thermal calcination process. The spectral characteristics and surface morphology were studied by XRD, FTIR and SEM anal-

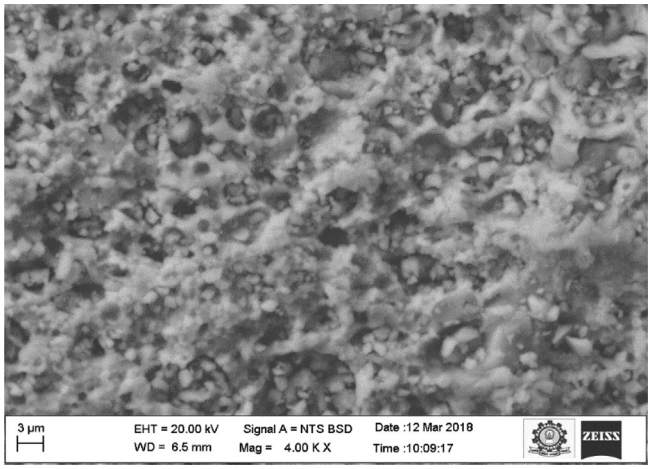

Fig. 6. SEM micrograph of Fighting cock bone HAp.

ysis. The lattice parameters, mean grain size, surface area, volume and degree of crystallinity were determined using XRD spectral data. In this spectral analysis, both samples exhibit hexagonal crystalline structure, but the mean crystallite size of Fighting cock bone HAp was smaller than Black Sumatra bone HAp. The FTIR spectrum revealed the presence of major constituent of bone carbonate, phosphate groups and the degradation of organic matters. SEM analysis exposed the porous nature of the bone HAp material of both bone samples. The comparative analysis concluded that the HAp obtained from Fighting cock bone was a capable biocompatible material for a coating material in bone implants and tissue engineering applications. Additionally, the use of waste chicken bones reduces the waste generation as well as avoids environmental pollution and also encourages the production of value added biomaterials for medical applications.

Declaration of Competing Interest

The authors declare that they have no known competing financial interests or personal relationships that could have appeared to influence the work reported in this paper.

Acknowledgement

We are grateful to the authorities of Kalasalingam Academy of Research and Education, Tamilnadu for providing facilities for instrumental analysis. The authors extend their appreciation to the Researchers supporting project number (RSP-2020/94) King Saud University, Riyadh, Saudi Arabia.

References

Adeogun, A.I., Ofudje, E.A., Idowu, M.A., Kareem, S.O., Vahidhabanu, S., Babu, B.R., 2018. Biowaste-derived hydroxyapatite for effective removal of Reactive Yellow 4 dye: equilibrium, kinetic, and thermodynamic studies. ACS Omega 3, 1991–2000.

Alif, M.F., Aprillia, W., Arief, S., 2018. A hydrothermal synthesis of natural hydroxyapatite obtained from *Corbicula moltkiana* freshwater clams shell biowaste. Mater. Lett 230, 40–43.

Balamurugan, A., Rebelo, A.H.S., Lemos, A.F., Rocha, J.H.G., Ventura, J.M.G., Ferreria, J. M.F., 2008. Suitability evaluation of sol-gel derived Si-substituted hydroxyapatite for dental and maxillofacial applications through in vitro osteoblasts response. Dent. Mater. 24, 1374–1380.

Barabas, R., Rogo, M., Sarkozi, M., Hoaghia, M.A., Cadar, O., 2019. Hydroxyapatite – Carbon nanotube composites for drug delivery applications. Braz. J. Chem. Eng. 36, 913–922.

Barakat, N.A.M., Khil, M.S., Omran, A.M., Sheikh, F.A., Kim, H.Y., 2009. Extraction of pure natural hydroxyapatite from the bovine bones biowaste by three different methods. J. Mater. Process. Technol. 209, 3408–3415.

Barua, E., Deogharea, A.B., Deba, P., Lala, S.D., Chatterjee, S., 2019. Effect of pre-treatment and calcination process on micro-structural and physico-chemical properties of hydroxyapatite derived from chicken bone bio-waste. Mater. Today: Proceedings 15, 188–198.

El Boujaady, H., Mourabet, M., El Rhilassi, A., Bennani-Ziatni, M., El Hamri, R., Taitai, A., 2016. Adsorption of a textile dye on synthesized calcium deficient hydroxyapatite (CDHAp): Kinetic and thermodynamic studies. J. Mater. Environ. Sci. 7, 4049–4063.

Gautier, H., Merle, C., Auget, J.L., Daculsi, G., 2000. Isostatic compression, a new process for incorporating vancomycin into biphasic calcium phosphate: comparison with a classical method. Biomaterials 21, 243–249.

Guimond-Lischer, S., Ren, Q., Braissant, O., Gruner, P., Wampfler, B., Maniura-Weber, K., 2016. Vacuum plasma sprayed coatings using ionic silver doped hydroxyapatite powder to prevent bacterial infection of bone implants. Biointerphases 11, 011012.

Harahap, H., Irany, Meldha, Z., 2017. Characterization of hydroxyapatite from chicken bone via precipitation. Key Eng. Mater. 744, 485–489.

Huang, J., Best, S.M., Bonfield, W., Buckland, T., 2010. Development and characterization of titanium-containing hydroxyapatite for medical applications. Acta. Biomater. 6, 241–249.

Hubaidillah, S.K., Othman, M.H.D., Tai, Z.S., Jamalludin, M.R., Yusuf, N.K., Ahmad, A., Rahman, M.A., Jaafar, J., Kadir, S.H.S.A., Harun, Z., 2020. Novel hydroxyapatite-based bio-ceramic hollow fiber membrane derived from waste cow bone for textile waste water treatment. Chem. Eng. J. 379, 122396.

Joschek, S., Nies, B., Krotz, R., Gopferich, A., 2000. Chemical and physicochemical characterization of porous hydroxyapatite ceramics made of natural bone. Biomaterials 21, 1645–1658.

Komlev, V.S., Barinov, S.M., Orlovskii, V.P., Kurdyumov, S.G., 2001. Porous ceramic granules of hydroxyapatite. Refract. Ind. Ceram. 42, 195–197.

Kumar, G.S., Girija, E.K., Venkatesh, M., Karunakaran, G., Kolesnikov, E., Kuznetsov, D., 2017. One step method to synthesize flower-like hydroxyapatite architecture using mussel shell bio-waste as a calcium source. Ceram. Int. 43, 3457–3461.

LeGeros, R.Z., 2002. Properties of soteoconductive biomaterials: calcium phosphates. Clin. Orthop. Relat. Res. 395, 81–98.

Londono-Restrepo, S.M., Jeronimo-Cruz, R., Rubio-Rosas, E., Rodriquez-Garcia, M.E., 2018. The effect of cyclic heat treatment on the physicochemical properties of bio hydroxyapatite from bovine bone. J. Mater. Sci: Mater. Med. 29, 52–57.

Luna-Zaragoza, D., Romero-Guzman, E.T., Reyes-Gutierrez, L.R., 2009. Surface and physicochemical characterization of phosphate vivianite. $Fe_2(PO_4)_3$ and hydroxyapatite, $Ca_5(PO_4)3OH$. J. Miner. Mater. Charact. Eng. 8, 591–609.

Mohd Puad, N.A.S., Koshy, P., Abdullah, H.Z., Idris, M.I., Lee, T.C., 2019. Synthesis of hydroxyapatite from natural sources. Heliyon. 5, 01588.

Mondal, S., Mondal, B., dey, A., Mukhopadhyay, S.S., 2012. Studies on processing and characterization of hydroxyapatite biomaterials from different bio wastes. J. Miner. Mater. Charact. Eng. 11, 55–67.

Murugan, R., Ramakrishna, S., 2005. Development of nanocrystals for bone grafting. Compos. Sci. Technol. 65, 2385–2406.

Murugan, R., Ramakrishna, S., Panduranga Rao, K., 2006. Nanoporous hydroycarbonate apatite scaffold made of natural bone. Mater. Lett. 60, 2844–2847.

Niakan, A., Ramesh, S., Ganesan, P., Tan, C.Y., Purbolaksono, J., Chandran, H., Ramesh, S., Teng, W.D., 2015. Sintering behavior of natural porous hydroxyapatite derived from bovine bone. Ceram. Int. 41, 3024–3029.

Ooi, C.Y., Hamdi, M., Ramesh, S., 2007. Properties of hydroxyapatite produced by annealing of bovine bone. Ceram. Int. 33, 1171–1177.

Palanivel, R., Rubankumar, A., 2013. Synthesis and spectroscopic characterization of hydroxyapatite by sol-gel method. Int. J. Chemtech. Res. CODEN (USA) 5, 2965–2969.

Pasteries, J.D., Womenka, B., Freeman, J.J., Rogers, K., Valsami-Jones, E., van der Houwen, J.A.M., Silva, M.J., 2004. Lack of OH in nanocrystalline apatite as a function of degree of atomic order; implications for bone and biomaterials. Biomaterials 25, 229–238.

Rajesh, R., Hariharasubramanian, A., Dominic, Y., 2012. Chicken bone as a bioresource for the bioceramic (Hydroxyapatite). Phosphorous Sulfur Silicon Relat. Elem. 187, 914–925.

Rajkumar, U., Haunshi, S., Paswan, C., Raju, M.V.L.N., Rama Rao, S.V., Chatterjee, R.N., 2017. Characterization of indigenous Aseel chicken breed for morphological, growth, production and meat composition traits from India. Poult. Sci. J. 96, 2120–2126.

Ramesh, S., Aw, K.L., Tolouei, R., Amiriyan, M., Tan, C.Y., Purbaloksono, J., Hassan, M. A., Teng, W., Hamdi, M., 2013. Sintering properties of hydroxyapatite powder prepared using different methods. Ceram. Int. 39, 111–119.

Ramesh, S., Loo, Z.Z., Tan, C.Y., Chew, W.J.K., Ching, Y.C., Tarlochan, F., Chandran, H., Krishnasamy, S., Bang, L.T., Shahan, A.A.D., 2018. Characterization of biogenic hydroyapatite derived from animal bones for biomedical applications. Ceram. Int. 44, 10525–10530.

Rezakhani, A., Motlagh, M.M.K., 2012. Synthesis and characterization of hydroxyapatite nanocrystal and gelatin doped with Zn^{2+} and cross linked by glutaraldehyde. Int. J. Phys. Sci. 7, 2768–2774.

Rivera-Munoz, E.M. 2011. Hydroxyapatite-Based Materials: Synthesis and Characterization, Biomedical Engineering - Frontiers and Challenges, Reza Fazel-Rezai, IntechOpen.

Ronan, K., Kannan, B.B., 2017. Novel sustainable route for synthesis of hydroxyapatite biomaterial from biowastes. ACS Sustain. Chem. Eng. 5, 2237–3345.
Senthilarasan, K., Ragu, A., Sakthivel, P., 2014. Synthesis and characterization of hydroxyapatite and gelatin doped with magnesium chloride for bone tissue engineering. Int. J. Eng. Res. Technol. 3, 917–920.
Sun, R., Chen, K., Liao, Z., Meng, N., 2013. Controlled synthesis and thermal stability of hydroxyapatite hierarchial microstructures. Mater. Res. Bull. 48, 1143–1147.
Supova, M., Martynkova, G.S., Sucharda, Z., 2011. Bioapatite made from chicken femur bone. Ceram-Silik. 55, 256–260.
Leventouri, Th., 2006. Synthetic and biological hydroxyapatites: crystal structure questions. Biomaterials. 27, 3339–3342.
Venkatesan, J., Kim, S.K., 2010. Effect of temperature on isolation and characterization of hydroxyapatite from Tuna (*Thunnus obesus*) bone. Materials 3, 4761–4772.
Villacampa, A.I., Garcia-Ruiz, J.M., 2000. Synthesis of a new hydroxyapatite – silica composite material. J. Crys. Growth. 211, 111–115.
Webster, T.J., Ergun, C., Doremus, R.H., Siegel, R.W., Bizios, R., 2002. Enhanced functions of osteoblasts on nanophase ceramics. Biomaterials 21, 1803–1810.
White, A.A., Best, S.M., 2007. Hydroxyapatite- carbon nanotube composite for biomedical applications: a review. Int. J. Appl. Ceram. Technol. 4, 1–14.
Wopenka, B., Pasteris, J.D., 2005. A mineralogical perspective on the apatite in bone. Mater. Sci. Eng:C. 25, 131–143.
Xiao, W., Sonny Bal, B., Rahaman, M.N., 2016. Preparation of resorbable carbonate-substituted hollow hydroxyapatite microspheres and their evaluation in osseous defects in vivo. Mater. Sci. Eng.C. Mater. Biol. Appl. 60, 324–332.
Yang, Y., Ong, J.L., Tian, J., 2002. Rapid sintering of hydroxyapatite by microwave processing. J. Mater. Sci. Lett. 21, 67–69.
Ye, H., Liu, X.Y., Hong, H.J., 2009. Characteristics of sintered titanium/hydroxyapatite biocomposite using FTIR spectroscopy. Mater. Sci. Mater. Med. 20, 843–850.